Electronic Journal of Biotechnology 32 (2018) 13–18

Contents lists available at ScienceDirect

Electronic Journal of Biotechnology

Research article

Enhanced apoptosis and inhibition of gastric cancer cell invasion following treatment with LDH@Au loaded Doxorubicin

Hu Zhao, Xueqin Zhang *

Department of Normal Surgical, Qujing First People's Hospital, Qujing, Yunnan, China

ARTICLE INFO

Article history:
Received 13 July 2017
Accepted 13 December 2017
Available online 20 December 2017

Keywords:
Anti-cancer
Doxorubicin
Drug delivery
Layered double hydroxide
LDH@Au
Nanodrug
Nanoparticle
Nanotechnology
Suppression of cancer cell invasion
Suppression of tumor growth
Tumor

ABSTRACT

Background: The suppression of cancer cell growth and invasion has become a challenging clinical issue. In this study, we used nanotechnology to create a new drug delivery system to enhance the efficacy of existing drugs. We developed layered double hydroxide by combing Au nanosol (LDH@Au) and characterized the compound to prove its function as a drug delivery agent. The anti-cancer drug Doxorubicin was loaded into the new drug carrier to assess its quality. We used a combination of apoptosis assays, cell cycle assays, tissue distribution studies, cell endocytosis, transwell invasion assays, and immunoblotting to evaluate the characteristics of LDH@Au as a drug delivery system.
Results: Our results show that the LDH@Au-Dox treatment significantly increased cancer cell apoptosis and inhibited cell invasion compared to the control Dox group. Additionally, our data indicate that LDH@Au-Dox has a better target efficiency at the tumor site and improved the following: cellular uptake, anti-angiogenesis action, changes in the cell cycle, and increased caspase pathway activation.
Conclusions: Our findings suggest the nano drug is a promising anti-cancer agent and has potential clinical applications.

1. Introduction

Gastric cancer is the third most common cause of cancer-related mortality worldwide, and the 5-year survival rate is less than 30% [1,2]. There is a high incidence rate in of gastric cancer in Asia. Surgical resection is currently the most effective treatment and chemotherapy has a crucial role following surgical resection [3,4,5]. Anthracycline treatment and the combination of paclitaxel and thymidine phosphorylase are the key chemotherapeutic options. However, these treatments have different complications. Thus, potent antitumor agents with limited toxicities are needed in the clinic. Doxorubicin (Dox) is a chemotherapeutic drug that induces cell senescence at a low concentration and can induce apoptosis at higher concentrations [6]. Approximately 10% of Dox-treated patients have a risk of developing cardiac complications. Therefore, improving the efficacy and reducing the toxicity of Dox could provide a new possible treatment option [7].

The medical application of nano materials has increased, and there have been several achievements in both disease diagnosis and therapy [8,9]. Gold nanoparticles (Au nanoparticles, AuNPs) are considered as promising candidate tools for nanobased medicines and can be used in biosensors, bioimaging, photothermal therapy, and targeted drug delivery. AuNPs have high chemical stability, well-controlled size, and surface functional properties. Thus, these compounds are emerging as promising agents for anti-cancer treatment [10,11].

Layered double hydroxide (LDH) has the general formula of $[M^1\_x2 + Mx3 + (OH)_2]$ $[Ax/n]$ mH_2O. These materials are highly biocompatible, show low toxicity and have satisfactory loading efficiency. Several previous studies reported that LDH has acceptable controlled-release properties, which make it a suitable tool for drug delivery [12,13,14].

In this study, we synthesized high-quality LDH and combined Au nanosol to form a new nano-carrier system (LDH@Au). LDH@Au can take full advantage of the two nano materials and performed better as a carrier of anti-cancer medicine. LDH@Au bound Dox (LDH@Au-Dox) using ionic-exchange and showed significantly improved antitumor efficacy in gastric carcinoma cells compared to the control drug.

2. Methods

2.1. Materials and cell culture

The gastric cancer cells SGC-7901 were obtained from the Institute of Cell Biology (Shanghai, China) and cultured in the RPMI-1640 medium (HyClone, MA, USA) with 10% deactivated fetal bovine serum

* Corresponding author.
E-mail address: xueqinzhang2017@163.com (X. Zhang).
Peer review under responsibility of Pontificia Universidad Católica de Valparaíso.

https://doi.org/10.1016/j.ejbt.2017.12.004

(FBS, Gibco, NY, USA) and 1% penicillin–streptomycin. The cells were incubated at 37°C with 5% CO_2.

2.1. Preparation of LDH, LDH@Au, and LDH@Au-DOX

The Mg–Al/LDH was synthesized by hydrothermal treatment. Briefly, Al $(NO_3)_3 \cdot 9H_2O$ (0.372 g, 0.002 M) and Mg $(NO_3)_2 \cdot 6H_2O$ (0.769 g, 0.006 M) were dissolved in 10 mL deionized ddH_2O and then the mixed salt solution was added into 40 mL NaOH (0.272) solution. The mixed solution was stirred at 60°C for 0.5 h in an N_2 atmosphere.

The solutions of $HAuCl_4 \cdot 4H_2O$ (2.44×10^{-3} mol/L), $Na_3C_6H_5O_7 \cdot 2H_2O$ (3.43×10^{-2} mol/L), polyvinylpyrrolidone (PVP, 1.00×10^{-4} mol/L) and $NaBH_4$ (0.391 mol/L) were pre-made for use.

We added 10 mL $HAuCl_4 \cdot 4H_2O$ solution to 80 mL ddH2O and stirred at 600 r/min for 2 min before heating to 75°C. A reducing agent ($Na_3C_6H_5O_7$ or $NaBH_4$) was quickly added into the mixed solution and heated for 9 min before stirring for 5 min. The mixed solution was cooled to room temperate, which led to the formation of Au nanosol.

The Mg–Al/LDH and Au nanosol were mixed in ddH_2O and stirred at room temperate in an N_2 atmosphere for 24 h. The LDH@Au composite nanomaterial was formed through anion exchange.

The Dox (10 mg) and LDH@Au (30 mg) were mixed in 20 mL deionized ddH_2O. The mixture was stirred at room temperate for 24 h and centrifuged twice. The supernatant was then removed and the precipitate was lyophilized to obtain the LDH@Au-Dox.

2.2. Transmission Electron Microscopy (TEM)

The surface morphology of LDH, Au, and LDH@Au was examined using a transmission electron microscope (JEOL, Tokyo, Japan). Drops of LDH, Au, and LDH@Au solutions were placed on the carbon-coated copper TEM grids (150 mesh, Ted Pella Inc., Rodding, CA, USA). The samples were observed at 100 kV under a microscope.

2.3. Size distribution by intensity study (DLS)

The size distribution of LDH@Au was determined by DLS. The LDH@Au (1 mg/mL) was prepared by diluting 100 μL samples in a 1-mL aqueous solution. The distribution was measured at 25°C by photon correlation spectroscopy (Zetasizer Nano ZS, Malvern Instruments, Malvern, UK).

2.4. Zeta potential

The zeta potential values of LDH@Au were measured based on the electrophoretic mobility using samples with concentrations (10 μg/mL) defined by photon correlation spectroscopy (Zetasizer Nano ZS, Malvern Instruments, Malvern, UK) at 25°C.

2.5. Cellular cytotoxicity

SGC-7901 cells were seeded into a 96-well plate at a density of 1×10^4/per well. The cells were incubated overnight and then treated with Dox, LDH@Au, and LDH@Au-Dox at various concentrations (0–4 μg/mL) for 24 h. The control group received no treatment. All the cells were incubated with 10 μL of 5 mg/mL 3-(4,5-dimethylthiazol-2-yl)-2,5-diphenyltetrazolium bromide (MTT) solution for 4 h at 37°C. Each well was then treated with 150 μL dimethyl sulfoxide (DMSO). The absorbance was measured at 490 nm using a microplate reader and the cell viability was calculated [15].

2.6. Cell cycle assay

Cell cycle status was measured in SGC-7901 cells treated with 3 μg/mL Dox or LDH@Au-Dox for 24 h. The cells were then fixed with 70% ethanol for 2 h. The control group received no treatment. The cells were then stained with propidium iodide (PI), and the cell cycle distribution was analyzed by flow cytometry [16].

2.7. Apoptosis assay

The in vitro apoptosis of SGC-7901 was analyzed by flow cytometry. Briefly, SGC-7901 cells were seeded onto 6-well plate at 1.5×10^6 cells per well and incubated overnight to form monolayer cells. The cells were divided into different groups and each group was incubated with LDH-Au, Dox, and LDH-Au-Dox at concentrations ranging from 0.5 μg/mL to 4.0 μg/mL or without any treatment (control) at 37°C for 24 h. The cells were collected and stained with Annexin V APC and PI before analysis by flow cytometry (Becton Dickinson, San Jose, CA).

2.8. Cell endocytosis and TEM observation of cellular uptake

Endocytosis was investigated by confocal microscopy (Leica TCS SP5, Leica Microsystems GmbH, Germany). SGC-7901 cells were seeded on confocal dishes at a concentration of 0.8×10^6 per plate and then incubated overnight to form monolayer cells. The cells were treated with either Dox or LDH@Au-Dox at same concentration (4.0 μg/mL) for 24 h. The cells were washed twice with PBS and stained with DAPI to localize the nuclei.

SGC-7901 cells were treated with different concentrations of LDH@Au-Dox for 2 h and centrifuged at 1000 r/min for 5 min to observe cellular uptake by TEM. The pellet was washed by PBS and fixed with 2% glutaraldehyde. Then, the cells were washed and evaluated using the TEM assay described in Section 2.2.

2.9. Tissue distribution

We subcutaneously injected 1×10^6 SGC-7901 cells in nude mice to form tumors. The xenograft animals were then treated with Dox or LDH@Au-Dox (10 mg/mL) by i.p. injection. The treated mice were sacrificed after 24 h. The organs and tumor tissue were homogenized and extracted. The drug level was measured by HPLC.

2.10. Transwell invasion assay

The Matrigel™ Matrix (BD Biosciences, San Jose, CA, USA) was diluted in serum-free medium and used to coat 24-well transwell inserts (BD Biosciences). SGC-7901 cells were serum-starved for 4 h and then collected and resuspended in 200 μL serum-free medium at a concentration of 1×10^5 cells with 5 μg/ml of LDH@Au, Dox, or LDH@Au-Dox. The cells were loaded into the upper chamber of the wells. We then placed 600 μL of medium containing 10% FBS in the lower chamber. The cells on the upper surface of the filters were gently removed and the invasive cells on the lower surface were fixed with ethanol after 24 h. The cells were stained with AM-calcein. We counted five fields for each group using a microscope [17].

2.11. Western blotting

SGC-7901 cells were treated with 4 μg/mL Dox or LDH@Au-Dox. The cells were collected and washed with PBS after 16 h. We then separated 20 μg of protein lysate by sodium dodecyl sulfate gel electrophoresis and transferred the proteins to PVDF membranes. The membranes were probed for β-actin, cytochrome-C, caspase-3, and caspase-9 (Cell Signaling Technology, MA, USA). The protein signals were detected using the ECL detection system and quantified by BandScan.

2.12. Statistical analysis

All data are expressed as the mean ± SD and analyzed with T-test. All values of $P < 0.05$ were considered statistically significant.

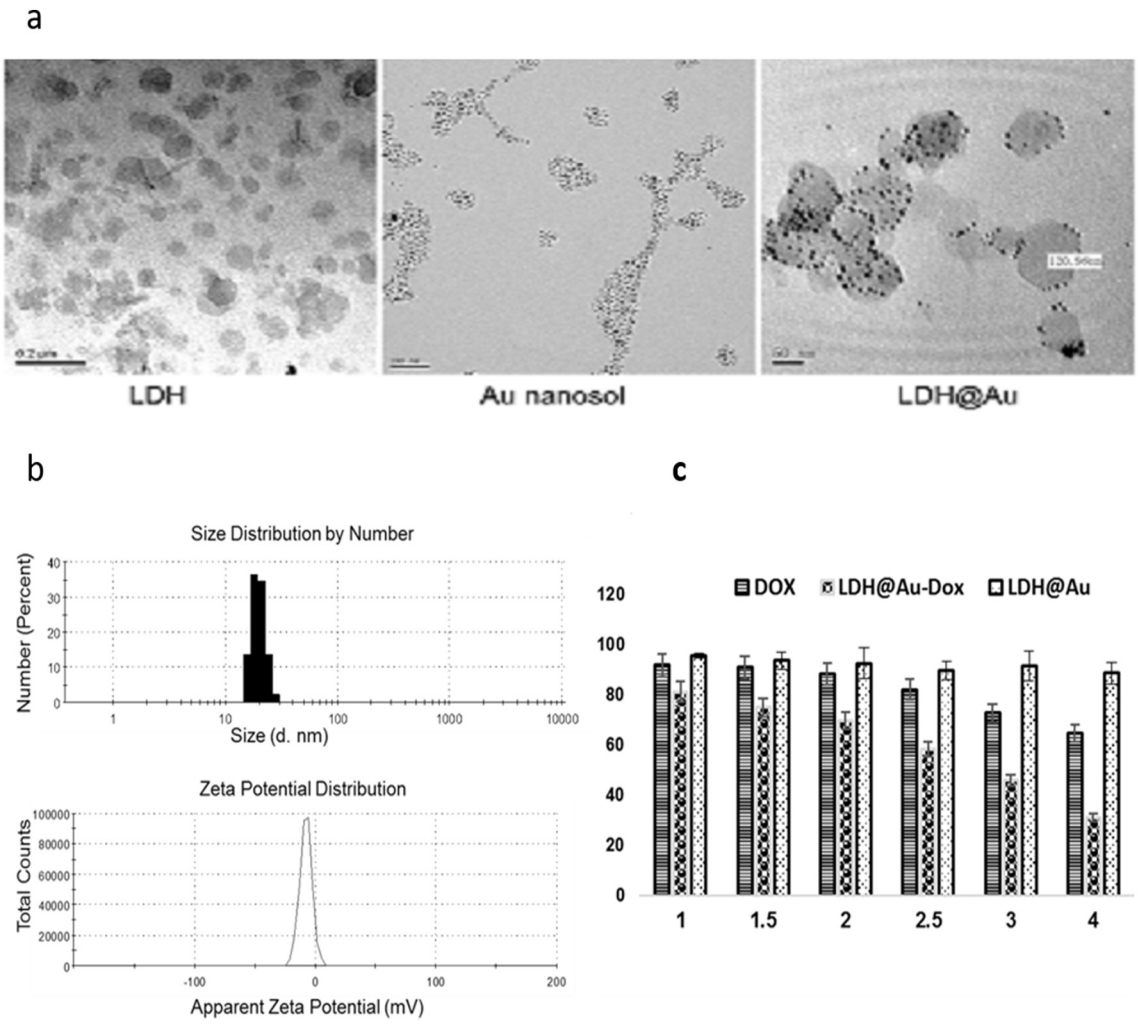

Fig. 1. (a) TEM images of LDH, Au nanosol, and LDH@Au, respectively. (b) Size distribution and Zeta potential of LDH@Au. (c) MTT analysis of SGC-7901 cell viability treated with Dox, LDH@Au, and LDH@Au-Dox after 24 h. Errors bar represent the means of three independent experiments.

3. Results

3.1. Physicochemical characterization of LDH@Au-Dox

The TEM images (Fig. 1a) showed the morphology of LDH, Au, and LDH@Au nanoparticles. The LDHs were plate-like hexagons approximately 60–120 nm in size. The Au nanosol was sol–gel with granulated Au nanoparticles smaller than 5 nm. The images also showed that Au nanoparticles were distributed on the edge of the hexagonal LDH, which are approximately 120 nm. The level of Au in LDH@Au was 10^{-5} mol/l. The presence of the diluted nanoparticle on the surface was measured by zeta potential (Fig. 1b). LDH@Au had a negative zeta potential of -12.3 mV $\pm$ 1.2 mV. The size of LDH@Au was determined using Distribution by Intensity Study (DLS). The DLS results for LDH@Au showed an average diameter of 118 nm and is consistent with the TEM findings. The PDI value is 0.232, which indicates a moderately appropriate polydispersion distribution of the nanoparticles.

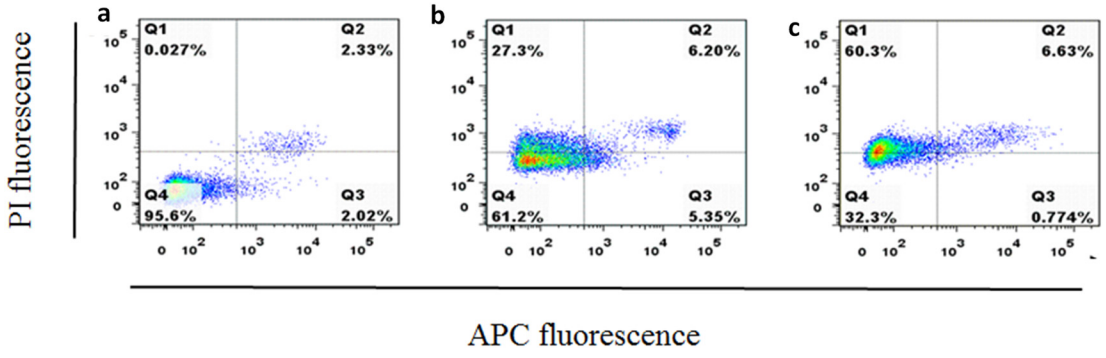

Fig. 2. Flow cytometry analysis of SGC-7901 cells with different treatments for 24 h. Cells were incubated with Control (a), Dox (b), and LDH-Au-Dox (c) at 37°C. The cells were collected and stained with Annexin V APC and PI before analysis by flow cytometry.

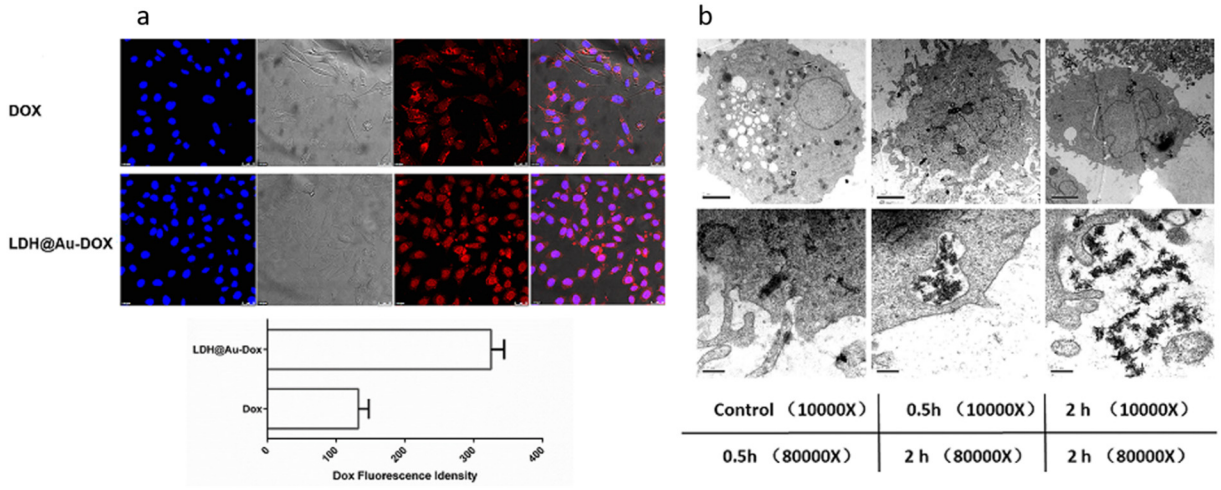

Fig. 3. (a) Cellular uptake of SGC-7901 cells treated with Dox and LDH-Au-Dox for 24 h. The cells were collected and stained with DAPI and imaged by confocal microscopy. Quantification of Dox fluorescence was calculated by ImageJ. (b) The cellular uptake observed by TEM.

3.2. LDH@Au-Dox introduces apoptosis of SGC-7901 cell

The apoptosis of treated SGC-7901 cells was measured by MTT assay and flow cytometry. The data in Fig. 1c, show more than 90% of cells survived after being treated with LDH@Au, and 57% cells survived in the group treated with 2.5 μg/mL. The MTT results show a clear increase of LDH@Au-Dox induced SGC-7901 death compared to Dox only treated cells. The data in Fig. 2 show that there is an enhanced cell growth inhibition activity of LDH@Au-Dox compared to Dox only. There were 67% dead or apoptotic cells after co-incubating cells with 4 μg/mL LDH@Au-Dox. However, there were only 36% apoptotic cells in the Dox treated group.

3.1. Cellular uptake of LDH@Au-Dox

The confocal images (Fig. 3a) indicated that there was cellular uptake of both LDH@Au-Dox and Dox alone. However, the cellular uptake in the LDH@Au-Dox group is higher than the Dox group.

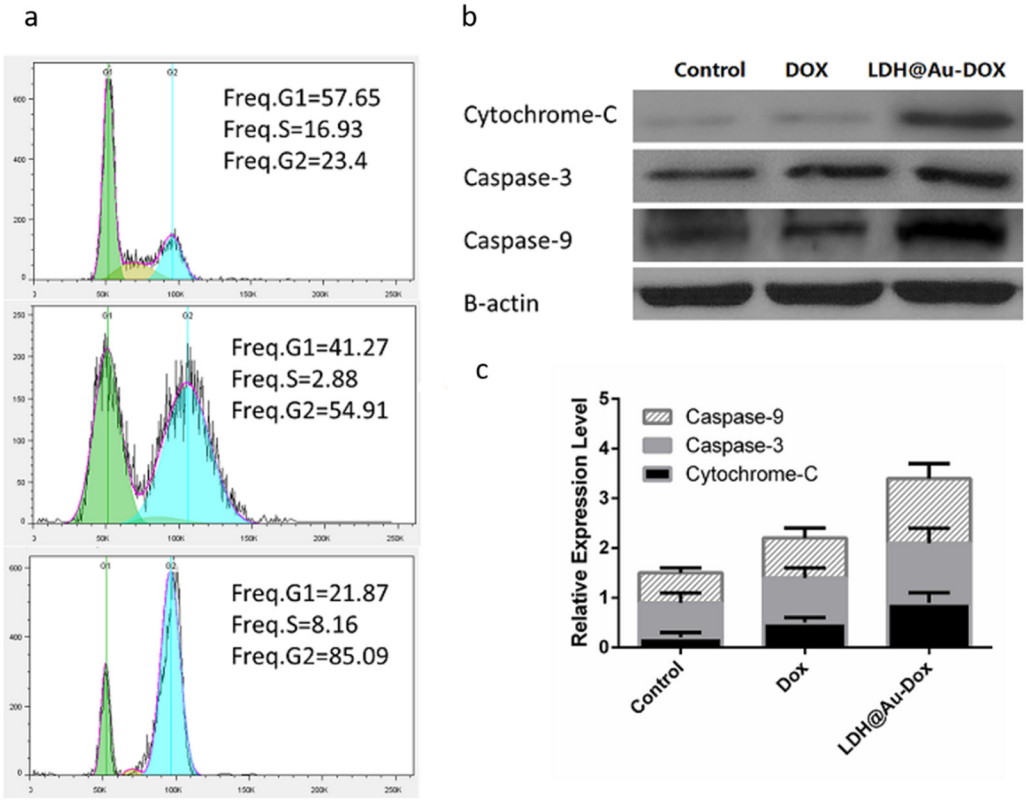

Fig. 4. (a) Cell cycle analysis of SGC-7901 cells treated with LDH@Au-Dox by FACS. (b) Western blot assay of the selected proteins expression. (c) Quantification of the expression in (b).

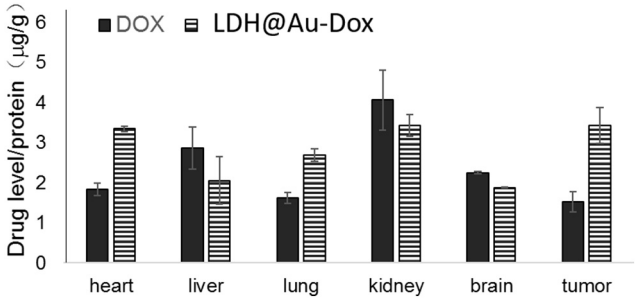

Fig. 5. The tissue distribution of Dox and LDH@Au-Dox 24 h after i.p. injection.

The TEM images (Fig. 3b) showed that LDH@Au-Dox was present in the cell cytosol and drug uptake is clearly time-dependent. After 2 h we observed LDH@Au-Dox in the nuclei of treated cells.

3.2. LDH@Au-Dox affects SGC-7901 cell proliferation and cytokinesis

The results in Fig. 4 show that the cell cycle was different after treatment with Dox and LDH@Au-Dox. The cells treated with Dox had 41.27% and 54.91% of cells in G1 and G2 phase, respectively. However, the LDH@Au-Dox group had only 21.87% cells in G1 phase and 85.09% cells in G2 phase. The immunoblotting results indicated that there was a significant increase of level of cytochrome c, caspase-3, and caspase-9 in the LDH@Au-Dox group.

3.3. LDH@Au-Dox targets to the tumor in vivo

The tissue distribution of LDH@Au-Dox was examined 24 h after a single treatment. The delivery effect of LDH@Au is obvious as the drug level is highly increased in the tumor tissue by the LDH@Au delivery system (Fig. 5).

3.4. Enhanced inhibition of gastric cancer metastasis in vitro

The impact of LDH@Au-Dox on SGC-7901 cell invasion was investigated by transwell migration assay. We found that there was an enhanced inhibition of invasion when the cells were treated with LDH@Au-Dox compared to the Dox treated group. The results also showed the LDH@Au treated group was significantly different than the untreated group (Fig. 6).

4. Discussion

LDH is a type of inorganic nano-material with a layered structure consisting of evenly distributed metal ions due to the minimum and orientation effect of the lattice energy. In each unit of the layered structure the chemical composition and structure remain unchanged [18,19,20]. Moreover, the anions distribute uniformly because of the layer charge attraction, interlayer ion exclusion, and limited space between layers. LDH could be suitable for drug delivery due to its characteristics and previous studies demonstrated LDH can improve the efficacy of loaded drug and reduce the toxicity. However, the LDH delivery system has a problem of targeting the site of action. Nano Au has a good targeting function and can be combined with LDH to form a better drug carrier [21,22]. LDH@Au has the advantages of both LDH nanoparticles and Au nanosol. Therefore, it can achieve both targeting and control releasing action to improve the bioavailability of loaded drug and in vivo circulation time.

We evaluated the properties of LDH@Au nanoparticles and found that they have a core–shell structure with an average size of 120 nm. The LDH@Au delivery system was used to load Dox and evaluate the function. We found that LDH@Au-Dox improved the level of drug at the tumor site and contributed to the cellular uptake of Dox. Moreover, compared to blank Dox group, the LDH@Au-Dox enhanced cell apoptosis and inhibited invasion. These findings suggest the addition of LDH@Au improves Dox function and suppresses tumor cell growth and migration. Many anti-cancer drugs try to improve tumor apoptosis and inhibit cancer metastasis [23]. Cancer metastasis is a major problem in the clinic and the majority of cancer-related deaths are due to metastatic disease [24,25].

We also investigated the mechanism of how LDH@Au-Dox functions and found SGC-7901 cells were in G2 phase after LDH@Au-Dox treatment. Additionally, and the expression level of cytochrome c, caspase-3, and caspase-9 indicates LDH@Au-Dox impacts caspase-dependent cytochrome c release. The activity of the caspase pathway is critical to the induction of apoptosis [26].

5. Conclusion

In this study, we synthesized and characterized LDH@Au nanoparticles and then loaded the particles with the anti-cancer drug Dox. The LDH@Au-Dox showed enhanced anti-cancer effects and both improved tumor cell apoptosis and inhibited cancer cell invasion. These characteristics of LDH@Au-Dox may be due to anti-angiogenic action and activation of the caspase pathways. Our work provides a

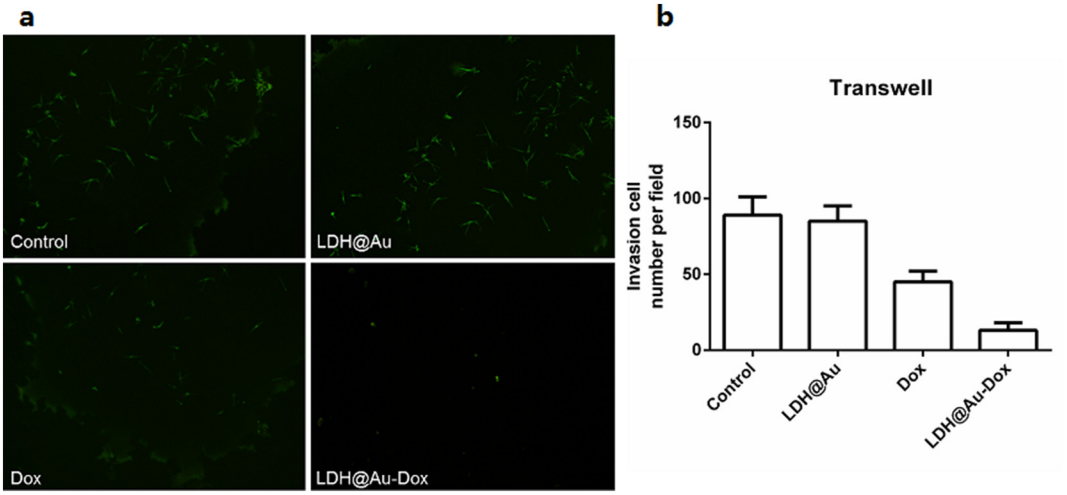

Fig. 6. Transwell invasion of SGC-7901 cell treated with 5 μg/mL of LDH@Au, DOX or LDH@Au-DOX for 24 h or untreated. (a) Representative images of treated and untreated cells are shown (40× magnification). The number of invading cells were was counted. (b) Quantification of the invasion cells in (a).

promising drug delivery system to solve the clinical anti-cancer problem.

Conflict of interest

The authors did not report any conflicts of interest.

References

[1] Hou CG, Luo XY, Li G. Diagnostic and prognostic value of serum MicroRNA-206 in patients with gastric cancer. Cell Physiol Biochem 2016;39(4):1512–20. doi: https://doi.org/10.1159/000447854.

[2] Zhuo C, Li X, Zhuang H, et al. Elevated THBS2, COL1A2, and SPP1 expression levels as predictors of gastric cancer prognosis. Cell Physiol Biochem 2016;40(6):1316–24. doi: https://doi.org/10.1159/000453184.

[3] Ang TL, Fock KM. Clinical epidemiology of gastric cancer. Singapore Med J 2014; 55(12):621–8. doi: https://doi.org/10.11622/smedj.2014174.

[4] Kitagawa Y, Fujii H, Mukai M, et al. The role of the sentinel lymph node in gastrointestinal cancer. Surg Clin North Am 2000;80(6):1799–809. doi: https://doi.org/10.1016/S0039-6109(05)70262-0.

[5] Takeuchi H, Kitagawa Y. Sentinel lymph node biopsy in gastric cancer. Cancer J 2015; 21(1):21–4. doi: https://doi.org/10.1097/PPO.0000000000000088.

[6] Bai J, Ma M, Cai M, et al. Inhibition enhancer of zeste homologue 2 promotes senescence and apoptosis induced by doxorubicin in p53 mutant gastric cancer cells. Cell Prolif 2014;4783:211–8. doi: https://doi.org/10.1111/cpr.12103.

[7] Espelin CW, Leonard SC, Geretti E, et al. Dual HER2 targeting with Trastuzumab and liposomal-encapsulated doxorubicin (MM-302) demonstrates synergistic antitumor activity in breast and gastric cancer. Cancer Res 2016;76(6):1517–27. doi: https://doi.org/10.1158/0008-5472.CAN-15-1518.

[8] Wicki A, Witzigmann D, Balasubramanian V, et al. Nanomedicine in cancer therapy: challenges, opportunities, and clinical applications. J Control Release 2015;200: 138–57. doi: https://doi.org/10.1016/j.jconrel.2014.12.030.

[9] Xu X, Ho W, Zhang X, et al. Cancer nanomedicine: from targeted delivery to combination therapy. Trends Mol Med 2015;21(4):223–32. doi: https://doi.org/10.1016/j.molmed.2015.01.001.

[10] Yu Q, Li J, Zhang Y, et al. Inhibition of gold nanoparticles (AuNPs) on pathogenic biofilm formation and invasion to host cells. Sci Rep 2016;6(1):26667. doi: https://doi.org/10.1038/srep26667.

[11] Jung YL, Park JH, Kim MI, et al. Label-free colorimetric detection of biological thiols based on target-triggered inhibition of photoinduced formation of AuNPs. Nanotechnology 2016;27(5):055501. doi: https://doi.org/10.1088/0957-4484/27/5/055501.

[12] Zuo H, Gu Z, Cooper H, et al. Crosslinking to enhance colloidal stability and redispersity of layered double hydroxide nanoparticles. J Colloid Interface Sci 2015;459:10–6. doi: https://doi.org/10.1016/j.jcis.2015.07.063.

[13] Sun J, Lei Y, Dai Z, et al. Sustained release of Brimonidine from a new composite drug delivery system for treatment of glaucoma. ACS Appl Mater Interfaces 2017;9(9): 7990–9. doi: https://doi.org/10.1021/acsami.6b16509.

[14] Ladewig K, Niebert M, Xu ZP, et al. Efficient siRNA delivery to mammalian cells using layered double hydroxide nanoparticles. Biomaterials 2010;31(7):1821–9. doi: https://doi.org/10.1016/j.biomaterials.2009.10.058.

[15] Hu CE, Du PZ, Zhang HD, et al. Long noncoding RNA CRNDE promotes proliferation of gastric cancer cells by targeting miR-145. Cell Physiol Biochem 2017;42(1): 13–21. doi: https://doi.org/10.1159/000477107.

[16] Liu JF, Nie XC, Shao YC, et al. Bleomycin suppresses the proliferation and the mobility of human gastric cancer cells through the Smad signaling pathway. Cell Physiol Biochem 2016;40(6):1401–9. doi: https://doi.org/10.1159/000453192.

[17] Zhang W, Liu Y, Li YF, et al. Targeting of Survivin pathways by YM155 inhibits cell death and invasion in oral squamous cell carcinoma cells. Cell Physiol Biochem 2016;38(6):2426–37. doi: https://doi.org/10.1159/000445594.

[18] Ladewig K, Xu ZP, Lu GQ. Layered double hydroxide nanoparticles in gene and drug delivery. Expert Opin Drug Deliv 2009;6(9):907–22. doi: https://doi.org/10.1517/17425240903130585.

[19] Minko T, Rodriguez-Rodriguez L, Pozharov V. Nanotechnology approaches for personalized treatment of multidrug resistant cancers. Adv Drug Deliv Rev 2013; 65(13–14):1880–95. doi: https://doi.org/10.1016/j.addr.2013.09.017.

[20] Oh JM, Park CB, Choy JH. Intracellular drug delivery of layered double hydroxide nanoparticles. J Nanosci Nanotechnol 2011;11(2):1632–5. doi: https://doi.org/10.1166/jnn.2011.3409.

[21] Dreaden EC, Mackey MA, Huang X, et al. Beating cancer in multiple ways using nanogold. Chem Soc Rev 2011;40(7):3391–404. doi: https://doi.org/10.1039/c0cs00180e.

[22] Huang X, Jain PK, El-Sayed IH, et al. Gold nanoparticles: interesting optical properties and recent applications in cancer diagnostics and therapy. Nanomedicine (Lond) 2007;2(5):681–93. doi: https://doi.org/10.2217/17435889.2.5.681.

[23] Ebos JM, Lee CR, Cruz-Munoz W, et al. Accelerated metastasis after short-term treatment with a potent inhibitor of tumor angiogenesis. Cancer Cell 2009;15(3): 232–9. doi: https://doi.org/10.1016/j.ccr.2009.01.021.

[24] Fidler IJ. The pathogenesis of cancer metastasis: the 'seed and soil' hypothesis revisited. Nat Rev Cancer 2003;3(6):453–8. doi: https://doi.org/10.1038/nrc1098.

[25] Jin X, Zhu Z, Shi Y. Metastasis mechanism and gene/protein expression in gastric cancer with distant organs metastasis. Bull Cancer 2014;101(1):1–12.

[26] Ilan N, Elkin M, Vlodavsky I. Regulation, function and clinical significance of heparanase in cancer metastasis and angiogenesis. Int J Biochem Cell Biol 2006; 38(12):2018–39. doi: https://doi.org/10.1016/j.biocel.2006.06.004.